Supporting Information

In-depth magnetic characterization of a [2x2] Mn(III) square grid using SQUID mangetometry, INS and high-field EPR spectroscopy.

Andreas Konstantatos†*, Robert Bewley‡, Anne L. Barra#, Jesper Bendix†, Stergios Piligkos†, Høgni Weihe†*

Materials and Measurements

All reagents were purchased commercially and used without further purification.

Single crystal X-ray diffraction data were collected on a Bruker D8 Venture diffractometer equipped with a Mo K_α (λ = 0.71073 Å) high brilliance IμS radiation source, a multilayer X-ray mirror, a PHOTON 100 CMOS detector and an Oxford Cryosystems low temperature device. Data collection was performed at a temperature of 123K. The crystal structure of **Mn_4** was solved with the olex2.solve structure solution program of the Olex2 package[1] by using Charge Flipping methods and refined with the olex2.refine[2] refinement package by using Gauss-Newton minimization. Non-hydrogen atoms were refined anisotropically, whereas hydrogen atoms were placed at calculated positions and were refined as riding atoms with isotropic displacement parameters.

Powder X-ray crystallographic data have been collected at room temperature on a Bruker D8 Advance Powder Diffractometer operating in 2θ-θ configuration using Cu Kα (λ = 1.54184 Å) radiation.

Magnetization measurements were performed on a Quantum-Design MPMS-XL SQUID magnetometer equipped with a 5T dc magnet. The polycrystalline sample was enclosed on a polycarbonate capsule in n-hexadecane. The temperature dependence of the DC magnetic susceptibility was determined by magnetization measurements from 2 K to 280 K in a DC field of 1000 Oe. All the data were corrected for diamagnetic contributions from the sample, the n-hexadecane and the sample holder by the means of Pascal's constants[3]. The data were fitted using the in-house "susc" software.

INS measurements were performed at the cold neutron multi-chopper spectrometer LET, at the ISIS center of the Rutherford Appleton Laboratory (Harwell Oxford, UK). Data reduction was performed using Mantid package[4]. Approximately 2 g of non-deuterated sample of **Mn_4** was loaded in a double wall cylindrical aluminum can and placed in a standard Orange cryostat. The intensities of the spectra were summed over the full Q range. The spectra were simulated using the in-house "ins" software.

EPR spectra have been measured on a home-made instrumentation set-up at the High Magnetic Field Laboratory (Grenoble, France). Measurements were performed on a polycrystalline sample of **Mn_4** compressed into a tablet in order to prevent crystal orientation in the magnetic field. The simulated spectra were computed using an in-house software.

X-ray diffractometry

Table S1. Crystallographic data and refinement parameters for **Mn_4**.

Identification code	Mn_4
Empirical formula	$C_{17.5}H_{18.5}MnN_{2.5}O_{4.5}$
Formula weight	781.59
Temperature/K	123
Crystal system	monoclinic
Space group	C2/c
a/Å	23.7556(14)
b/Å	12.9539(8)
c/Å	22.6368(12)
α/°	90
β/°	108.793(2)
γ/°	90
Volume/Å^3	6594.6(7)
Z	8
ρ_{calc}g/cm^3	1.5743
μ/mm^{-1}	0.832
F(000)	3239.0
Crystal size/mm^3	0.112 × 0.071 × 0.018
Radiation	Mo Kα (λ = 0.71073)
2Θ range for data collection/°	4.32 to 50.06
Index ranges	-28 ≤ h ≤ 28, -15 ≤ k ≤ 15, -25 ≤ l ≤ 26
Reflections collected	44496
Independent reflections	5825 [R_{int} = 0.0923, R_{sigma} = 0.0456]
Data/restraints/parameters	5825/0/465
Goodness-of-fit on F^2	1.070
Final R indexes [I>=2σ (I)]	R_1 = 0.0367, wR_2 = 0.0802
Final R indexes [all data]	R_1 = 0.0587, wR_2 = 0.0896
Largest diff. peak/hole / e Å^{-3}	0.64/-0.48

Table S2. Selected bond distances and angles from the crystal structure of **Mn_4**.

Bond distances or angles	Value
Mn1 – O3	1.915(2) Å
Mn1 – O10	1.890(2) Å
Mn1 – O4	2.271(2) Å
Mn1 – O6	2.421(2) Å
Mn1 – O5	1.873(2) Å
Mn1 – N11	1.996(2) Å
Mn2 – O3	2.367(2) Å
Mn2 – O6	1.928(2) Å
Mn2 – O7	1.885(2) Å
Mn2 – O8	2.240(2) Å
Mn2 – O9	1.899(2) Å
Mn2 – N15	2.013(2) Å
Mn1 – O3 – Mn2	125.51(8)°
Mn1 – O6 – Mn2	126.60(9)°
O4 – Mn1 – O6	161.43(7)°
O3 – Mn2 – O8	162.37(7)°

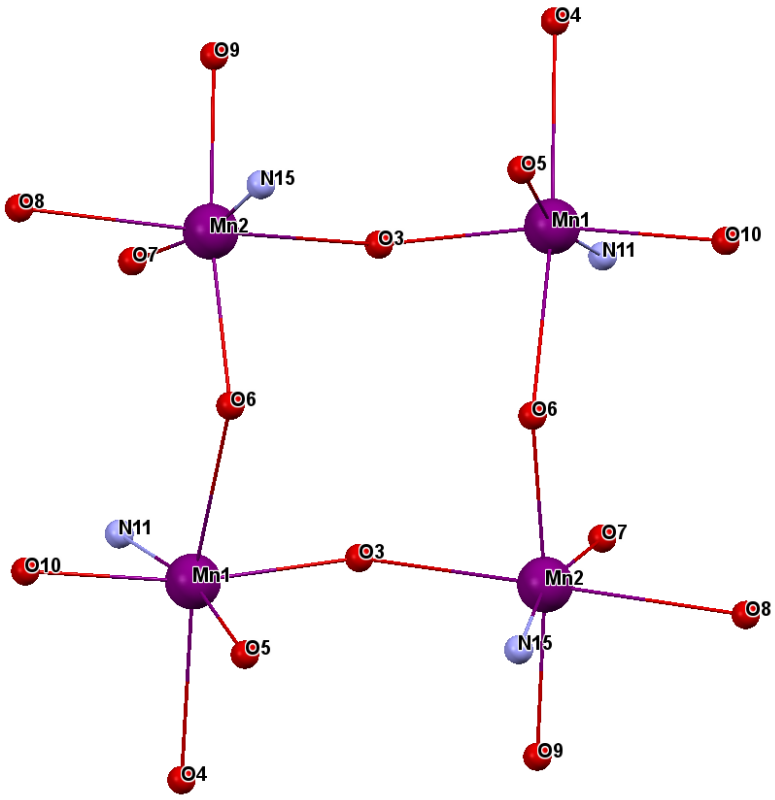

Figure S1. View of the magnetic core of **Mn_4** along the b axis (also the 2-fold proper rotation axis). Mn(III) ions are depicted as deep purple spheres, whereas the ligand environment around them is visualized as red spheres for oxygen

atoms and light blue spheres for nitrogen atoms. All other atoms have been intentionally omitted.

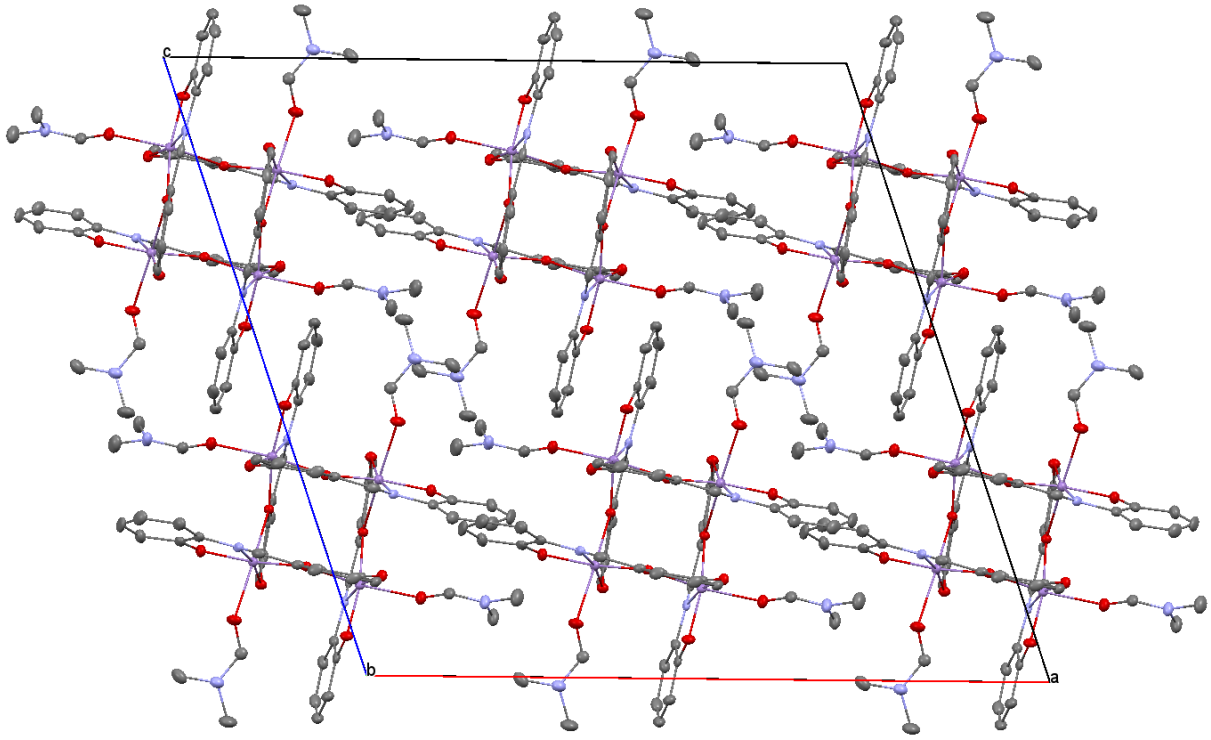

Figure S2. View along the *b* axis of the crystal packing of **Mn$_4$** molecules in the unit cell.

Bond valence sums

Bond valence sums have been calculated for the two crystallographically independent Mn(III) centers of **Mn$_4$** in order to verify their oxidation state. Table S3 summarizes the results of the calculations for all possible oxidation state combinations.

Table S3. Valence bond sums calculations for centres Mn1 and Mn2 of complex **Mn$_4$**[5,6]. The colors indicate the possible combinations of oxidation numbers.

		Oxidation state		
		II	III	IV
Metal centre	Mn1	3.4032	3.3818	3.3560
	Mn2	3.3568	3.3463	3.3116

Powder X-ray diffractometry

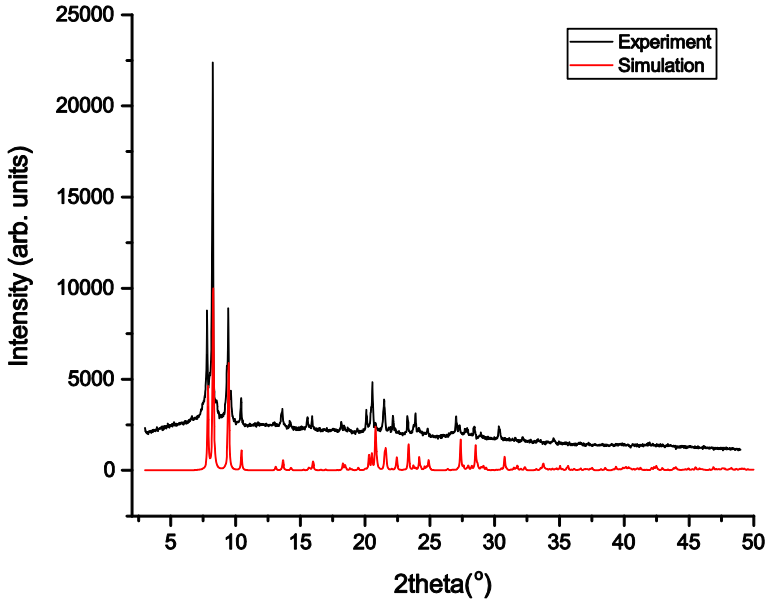

Figure S3. Powder diffractogram for complex Mn_4. The black line represents the experimental data collected at room temperature. The red line is simulated from the single crystal data collected at 123K.

Magnetic studies

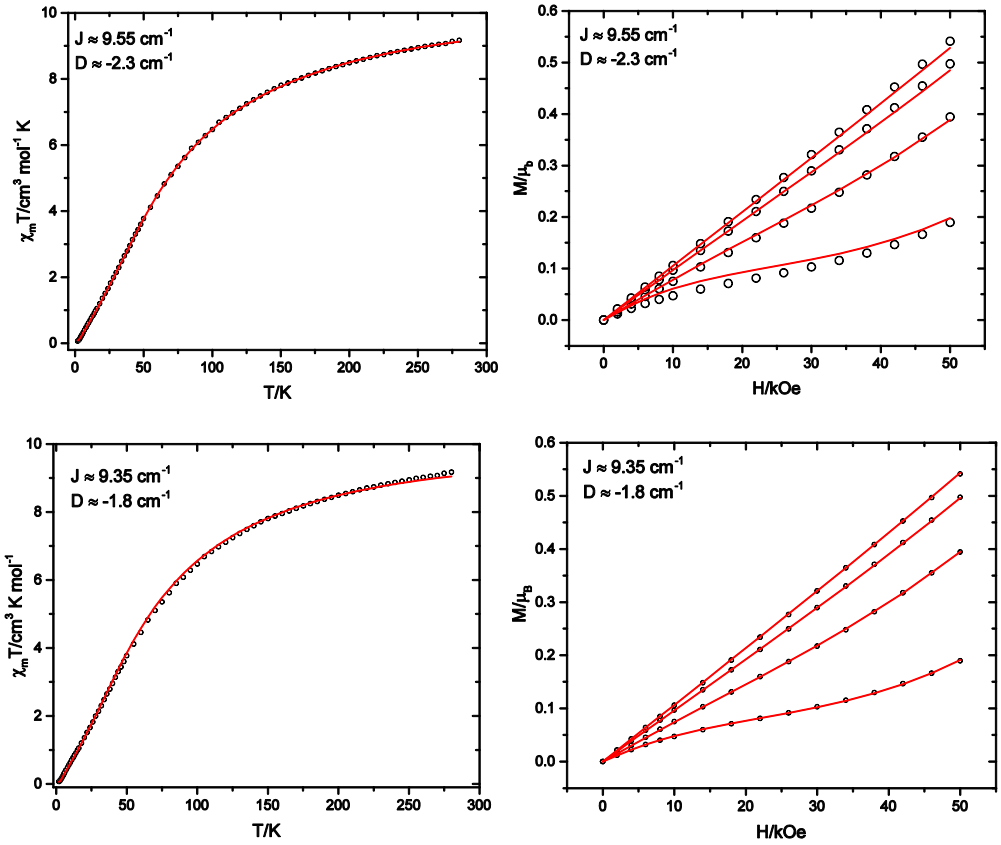

Fig S4. Fit of the $\chi_m T$ vs T and M vs H data to a one-J and one-D model, weighed towards the susceptibility data (top) and the magnetization data (bottom).

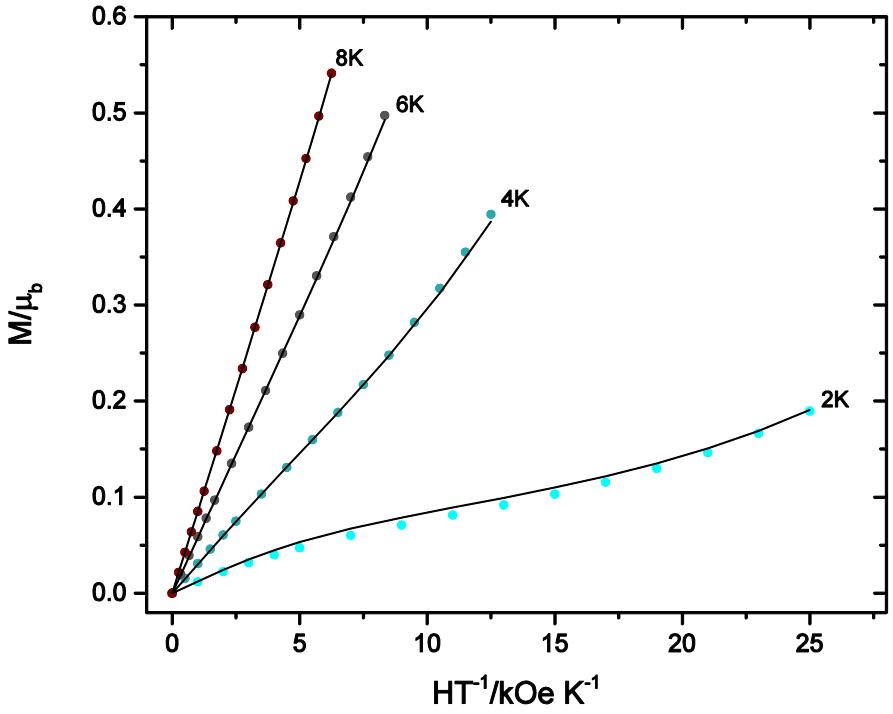

Figure S5. Reduced magnetization M vs HT^{-1} plot at different temperatures. Black solid lines are the best fit to the model described in the text.

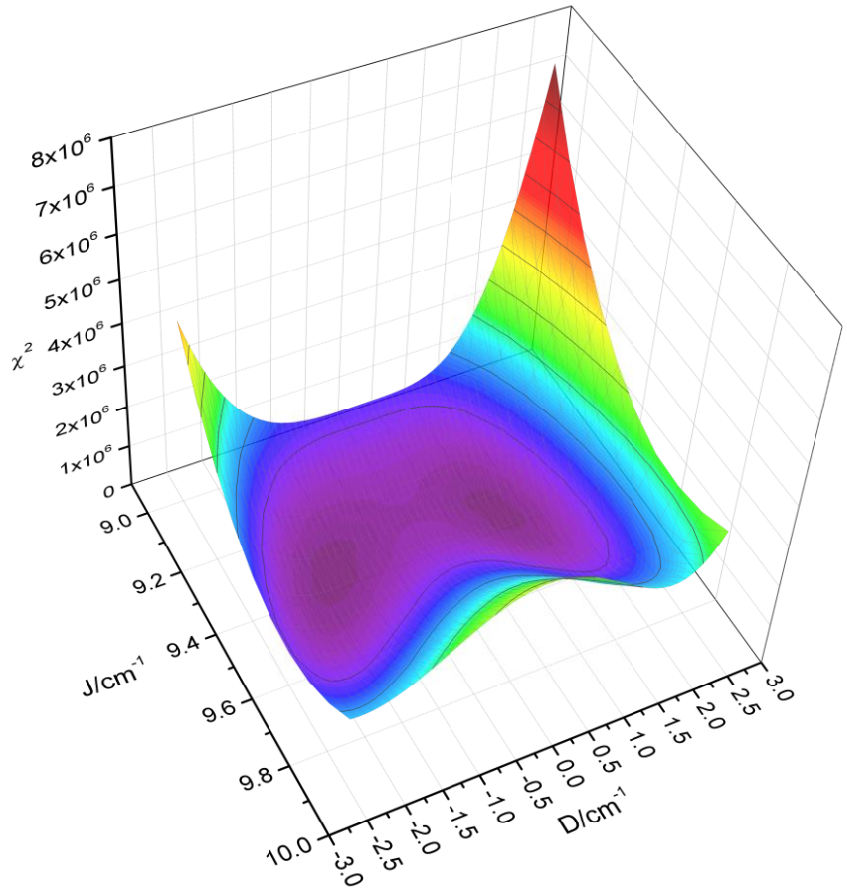

Figure S6. 3D surface graph of χ^2 in a range of D and J values.

Inelastic Neutron Scattering

Table S4. Incident energies and their respective resolutions for two different chopper speed setups.

Resolutions per energy					
energy	wavelength	resolution	energy	wavelength	resolution
17.4 meV	2.17 Å	950 µeV	59.4 meV	1.17 Å	860 µeV
5.5 meV	3.85 Å	170 µeV	10 meV	2.86 Å	215 µeV
2.67 meV	5.53 Å	60 µeV	3.96 meV	4.54 Å	57 µeV
1.57 meV	7.21 Å	27.5 µeV	2.11 meV	6.22 Å	22.5 µeV
1.03 meV	8.91 Å	14 µeV	1.31 meV	7.90 Å	11.5 µeV
Chopper speed 100 Hz			Chopper speed 200 Hz		

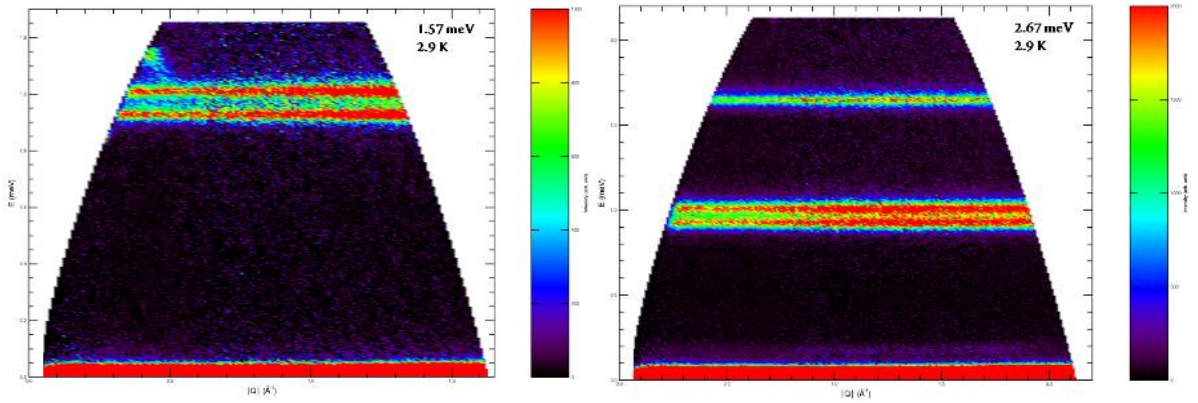
1.57 meV
2.9 K
2.67 meV
2.9 K

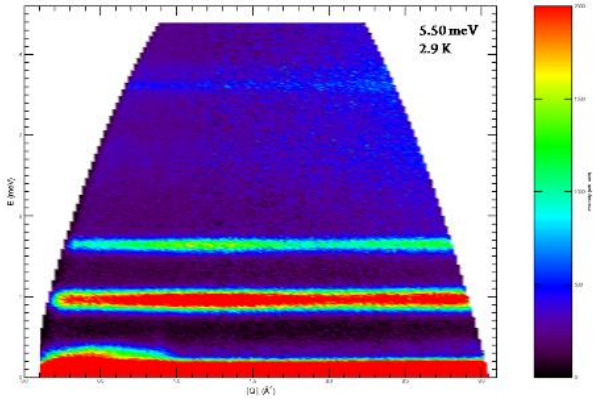
5.50 meV
2.9 K

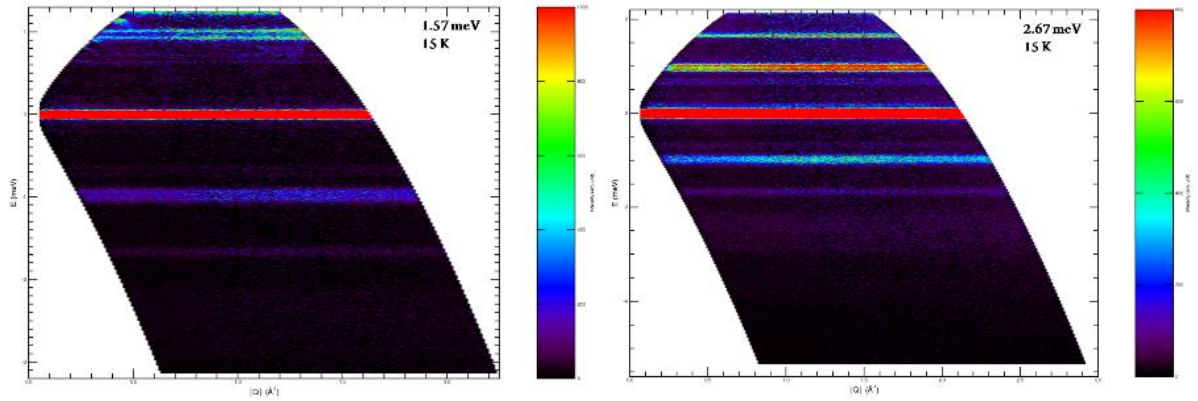
1.57 meV
15 K
2.67 meV
15 K

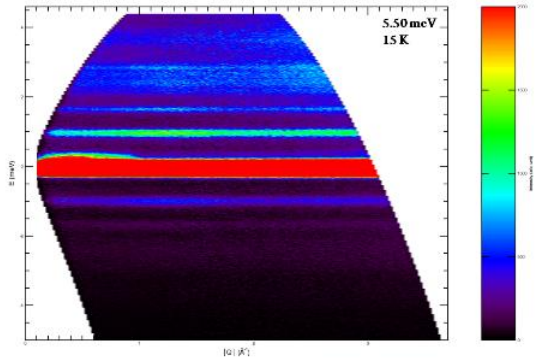
5.50 meV
15 K

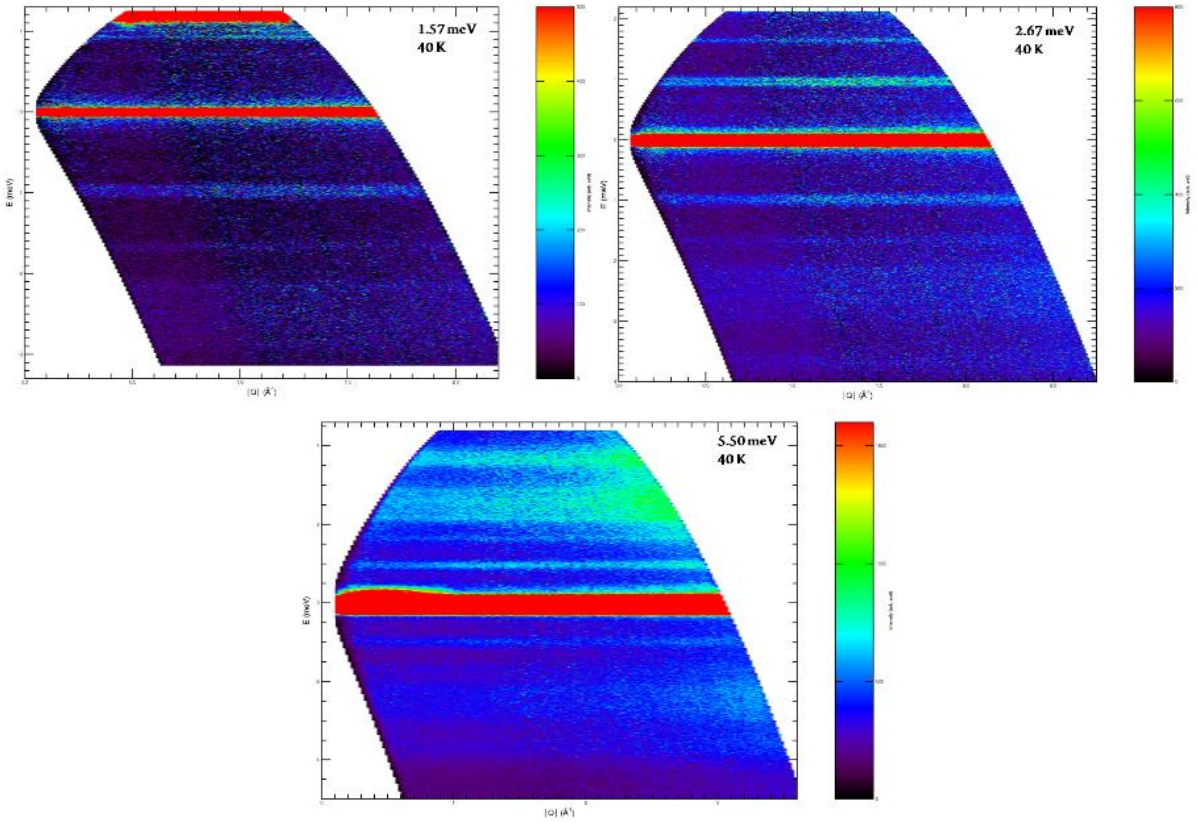

Figure S7. S(|Q|,E) maps for **Mn_4** obtained at different temperatures with several incident energies.

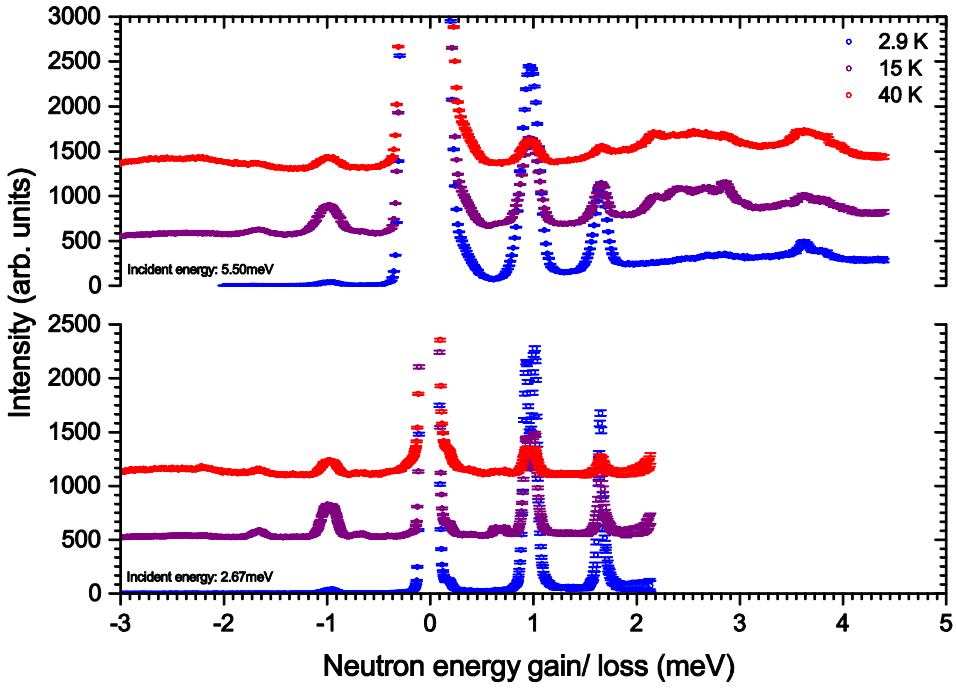

Figure S8. INS spectra at different incident energies and temperatures. The abscissa shows both energy gain and energy loss.

References

(1) Dolomanov, O. V.; Bourhis, L. J.; Gildea, R. J.; Howard, J. A. K.; Puschmann, H. *J. Appl. Crystallogr.* **2009**, *42* (2), 339–341.

(2) Bourhis, L. J.; Dolomanov, O. V.; Gildea, R. J.; Howard, J. A. K.; Puschmann, H. *Acta Crystallogr. Sect. A Found. Crystallogr.* **2015**, *71* (1), 59–75.

(3) Bain, G. a.; Berry, J. F. *J. Chem. Educ.* **2008**, *85* (4), 532.

(4) Arnold, O.; Bilheux, J. C.; Borreguero, J. M.; Buts, A.; Campbell, S. I.; Chapon, L.; Doucet, M.; Draper, N.; Ferraz Leal, R.; Gigg, M. A.; Lynch, V. E.; Markvardsen, A.; Mikkelson, D. J.; Mikkelson, R. L.; Miller, R.; Palmen, K.; Parker, P.; Passos, G.; Perring, T. G.; Peterson, P. F.; Ren, S.; Reuter, M. A.; Savici, A. T.; Taylor, J. W.; Taylor, R. J.; Tolchenov, R.; Zhou, W.; Zikovsky, J. *Nucl. Instruments Methods Phys. Res. Sect. A Accel. Spectrometers, Detect. Assoc. Equip.* **2014**, *764*, 156–166.

(5) Brown, I. D.; Gillespie, R. J.; Morgan, K. R.; Tun, Z.; Ummat, P. K. *Inorg. Chem.* **1984**, *23* (26), 4506–4508.

(6) Liu, W.; Thorp, H. H. *Inorg. Chem* **1993**, *32* (8), 4102–4105.